Hydrology
Current Research
ISSN: 2157-7587

Menna, Hydrol Current Res 2017, 8:2
DOI: 10.4172/2157-7587.1000276

Research Article Open Access

# Simulation of Hydro Climatological Impacts Caused by Climate Change: The Case of Hare Watershed, Southern Rift Valley of Ethiopia

**Biniyam Yisehak Menna***

*Department of Meteorology and Hydrology, College of Natural Sciences, Arba Minch University, Arba Minch, Ethiopia*

## Abstract

Ethiopia will be more vulnerable to climate change. Because of the less flexibility to adjust the economic structure and being largely dependent on agriculture, the impact of climate change has far reaching implication in Ethiopia. Simulation models of watershed hydrology and water quality are extensively used for water resources planning and management. The study aims to Simulate Hydro Climatological impacts caused by Climate Change: the case of Hare Watershed, Southern Rift Valley of Ethiopia. In the study the daily data values of rainfall and discharge for the current period of 1980-2006 were used. Historical Representative Concentration Pathway (RCPs) data of precipitation and temperature were used to extract raw climate variables. The raw RCPs data were corrected using a bias correction method. The downscaled climate data such as, RCP4.5 and RCP8.5 scenarios was used for the future period assessment. Soil water assessment tool (SWAT) models were used to Simulate Hydro Climatological impacts caused by Climate Change. Calibration and validation of the model output were performed by comparing predicted streamflow with corresponding measurements from the Hare river outlet for the periods 1991-2002 for calibration and 2003-2006 for validation. The models' calibration results show a good agreement with the observed flow with the coefficient of determination is 0.85 and a Nash Sutcliffe efficiency is 0.73. The result of mean monthly percentage changes of climate variables from the baseline period were used to simulate future projections of stream flow. Stream flow projections for future time periods showed that mean monthly stream flow may increase by 12.2, 8.0, and 13.9% at 2020s, 2050s, and 2080s, respectively, from the baseline period for RCP4.5 scenario, whereas for RCP8.5 scenario, it will be expected to increase by 7.3, 13.4, and 15.4% for 2020s, 2040s, and 2080s, respectively. The model simulations considered only future climate change scenarios assuming all spatial data constant. But change in land use scenarios other climate variables will also contribute some impacts on future stream flow.

**Keywords:** Climate change; Climate projection; RCPs; Streamflow; Bias correction; Hare watershed

## Introduction

Climate change refers to any systematic change in the long-term statistics of climate elements (such as temperature, pressure, or winds) sustained over several decades or longer time periods. Climate change describes changes in the global temperature over time (i.e., increase in global temperature or global warming) and its consequences on other climatic variables, such as pressure, humidity, wind etc. Observations that delineate how global temperature has increased in the past shows, the global average surface temperature have increased by 0.74°C/ Century [1].

The impact of climate change on water resources are the most crucial research agenda in worldwide level [2]. This change in climate causes a significant impact on the water resource by disturbing the normal hydrological processes. Future change in overall flow magnitude, variability and timing of the main flow event are among the most frequently cited hydrological issues [3,4].

The IPCC findings indicate that developing countries, such as Ethiopia, will be more vulnerable to climate change. It may have far reaching implications to Ethiopia for various reasons, mainly as its economy largely depends on agriculture and low adoptive coping. A large part of the country is arid and semiarid, and is highly prone to drought and desertification. Climate change and its impacts are, therefore, a case for concern to Ethiopia. Hence, assessing vulnerability to climate change impact mapping and preparing adaptation options as part of the national program is very crucial for the country [5].

In spite of the fact that the impact of different climate change scenarios is projected at global scale, the exact type, and magnitude of the impact at catchment scale is not investigated in most parts of the world. Hence, identifying local impact of climate change at watershed level is quite important. The economy of Ethiopia mainly depends on agriculture, and this in turn largely depends on available water resources. Given that a large part of the country is arid and semiarid and highly prone to drought and desertification, this represents a significant risk. Also, the country has a fragile highland ecosystem that is currently under stress due to increasing population pressure. Hare watershed is one of tributaries of Lake Abaya and high competition for irrigation water used among upstream and downstream irrigation sites. In addition, it can be considered as representative watershed where there is high landscape and climatic zone different with in short distance [6].

Therefore, the effect of climate change on water availability (with respect to water resource analysis, management, and policy formulation in the country) in the Hare watershed have not been adequately addressed. Hence, it is necessary to improve our understanding of problems involved to the change in climate.

In this climate change impact study, soil water assessment tool (SWAT) model was used. The framework of this approach is, firstly representative concentration pathway (RCPs) and then downscale or

***Corresponding author:** Biniyam Yisehak Menna, Department of Meteorology and Hydrology, College of Natural Sciences, Arba Minch University, PO Box 21, Arba Minch, Ethiopia, Tel: +251912444435; E-mail: b1n1y21@gmail.com

**Received** February 06, 2017; **Accepted** May 16, 2017; **Published** May 22, 2017

**Citation:** Menna BY (2017) Simulation of Hydro Climatological Impacts Caused by Climate Change: The Case of Hare Watershed, Southern Rift Valley of Ethiopia. Hydrol Current Res 8: 276. doi: 10.4172/2157-7587.1000276

correct RCPs data. Next feed the downscaled or corrected RCPs data into calibrated and validated hydrological models. After that, simulate streamflow for three future periods considering the climate change scenario. Finally, carry out hydro climatological impacts caused by climate change.

## Study Area and Dataset

### Study area

The study area, Hare River watershed, is located in the Abaya-Chamo sub-basin of the southern Ethiopian Rift Valley and drains to Lake Abaya, which is the second largest lake of the country. The watershed is situated between 37° 27' and 37° 37' Eastern longitude and 6° 03' and 6° 18' Northern latitude and has a land area of 153 km$^2$. The topography of the study area is generally increasing in elevation from the downstream to the upstream. The middle reach of the watershed is mainly covered by steep slopes characterized through abrupt faults [7].

The climate of the Hare watershed ranges from tropical to alpine due to its great difference in altitude and topographical elevation. The average annual temperature is 23°C and 14°C, and mean annual rainfall are 750 mm and 1300 mm at the lowland and highland respectively. Generally, about 55.56% is Dega (Humid), 22.84% is Woyna Dega (Sub-humid), 11.73% is Wurch (Alpine) and 9.25% is Kola (Sub-arid). The lower watershed area is characterized by dry Kola while the middle part of the watershed is characterized by moist woyna-dega and much of the area in the northern part is dominated by Dega and the tip is Wurch. The main and small rainy seasons at Hare watershed occur from April-May and September and October respectively. The spatial rainfall distribution at Hare watershed indicates that major increase of rainfall takes place with an increase in elevation from 1180 m up to 3,480 m above sea level (a.s.l.) [6] (Figure 1).

### Dataset meteorological data

Required long year daily precipitation data were collected from three meteorological stations such as, Arba Minch, Chencha, and Mirab Abaya. Daily maximum and minimum temperature data were collected from Arba Minch station. The historical weather data for above three station were obtained from National Meteorological Service Agency (NMSA) from 1980 to 2006 (Figure 2).

### Downscaled RCPs data

The Intergovernmental Panel for Climate Change (IPCC) has published projections of future climate change scenarios in a series of reports. There was a fundamental change between the fourth and fifth assessment reports (AR4 and AR5) [8-10] and in order to reflect such differences as well as model variability, the study looked at two future scenarios. The first scenario considers what the future climate will be under conditions with a representative concentration path (RCP) that assumes that radiative forcing will stabilize at 8.5 W/m$^2$ in 2100 (RCP8.5); the second less extreme scenario assumes that radiative forcing will stabilize at 4.5 W/m$^2$ in 2100 (RCP4.5).

Downscaled rainfall, and average, minimum and maximum temperatures for the period 1951-2100 have been obtained from CORDEX-Ethiopia database. The data correspond to three RCP scenarios- RCP2.6, RCP4.5, RCP6 and RCP8.5. In order to best conduct a future climate change study, RCP 4.5 and RCP 8.5 forced scenarios were selected from 2010 to 2100 for 3 climate stations, and downscaled to the same climate stations which were used for SWAT model for the hydro Climatological simulations (Table 1).

### Hydrological data

Stream flow was used for calibrating and validating the SWAT model simulation. Daily stream flow data were obtained from Ministry of Water Irrigation and Energy (MWIE) for Hare River from 1980 to 2006.

### Spatial data

Digital elevation model (DEM), land use/land cover, and soil are the three spatial data inputs required by SWAT model. DEM describes the elevation of any point in a given area at a specific spatial resolution as a digital file. DEM is one of the essential inputs required by SWAT: (1) to delineate the watershed into a number of sub-watersheds or sub-basins and (2) to analyze the drainage pattern of the watershed, slope, stream length, width of channel within the watershed. The DEM was obtained from USGS website with a resolution of 30 m by 30 m.

The land use map of the study area ware downloaded from USGS website with path-169 and row-056, 20 January 2000 satellite image. It has 8-bands, and with special resolution of 30 m × 30 m processed in ArcGIS was used for the hydrologic study input data. The land use of the area has reclassified based on the available topographic map, Arial photography and satellite images. The reclassification of land use map was done to represent the land use according to the specific land cover types such as type of Forest land, Water body, Cultivated land, Bush land and Bare land.

SWAT model requires different soil textural and physico-chemical properties such as soil texture, available water content, hydraulic conductivity, bulk density and organic car-bon content for different layers (up to 3 layers) of each soil type. These data were obtained mainly from the following sources: Ministry of Agriculture (MoA) and Africa CD-ROM (Food and Agriculture Organization of the United Nations [11], Major Soils of the world CD-ROM [12], Digital Soil Map of the World and Derived Soil Properties CD-ROM [13], Proper-ties and Management of Soils of the Tropics CD-ROM [14] (Figure 3).

## Methodology

This study, applying bias correction method for downscaled climate variables (precipitation and temperature) is the first and basic step for this impact assessment to be described. Stream flow modeling with SWAT is the second step in the methodology. Finally, climate change impact study using hydrological model is the subject to be discussed.

### Bias correction method of downscaled climate data

Often, the downscaled RCPs data cannot be directly used for impact assessment as the computed variables may differ systematically from the observed ones. Bias correction is therefore applied to compensate for any tendency to overestimate or underestimate the mean of downscaled variables. Bias correction factors are computed from the statistics of observed and simulated variables [15]. Two bias correction methods were tried in this study. First, the nonlinear bias correction method proposed by Nader et al. [16] and the second method called "delta approach". The formulas used for rainfall and temperature bias correction are indicated in Equations 1 and 2. Corrections factors were computed for each month.

### Precipitation correction

In the bias correction technique, nonlinear correction each daily

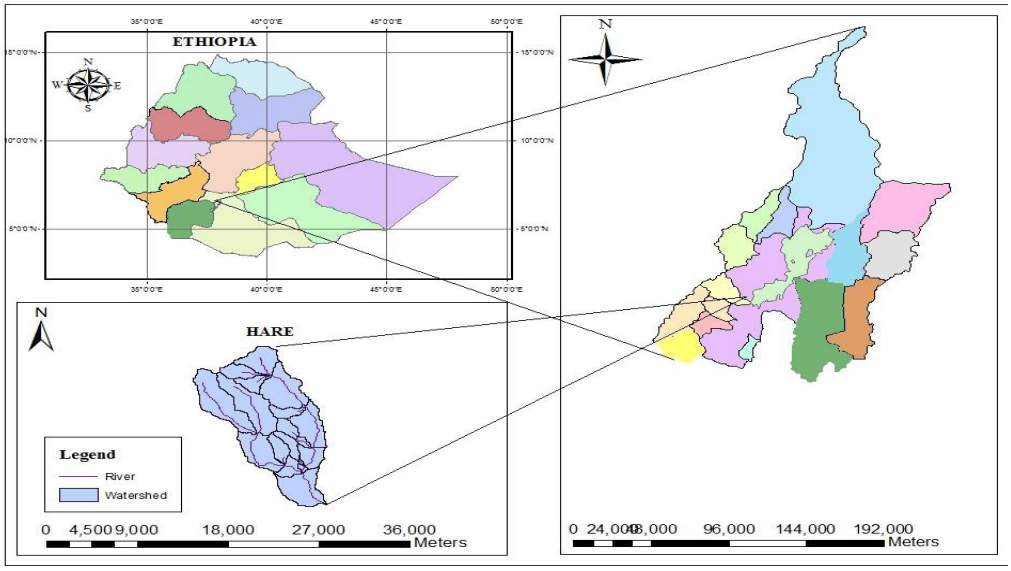


**Figure 1:** Location of Hare Watershed.

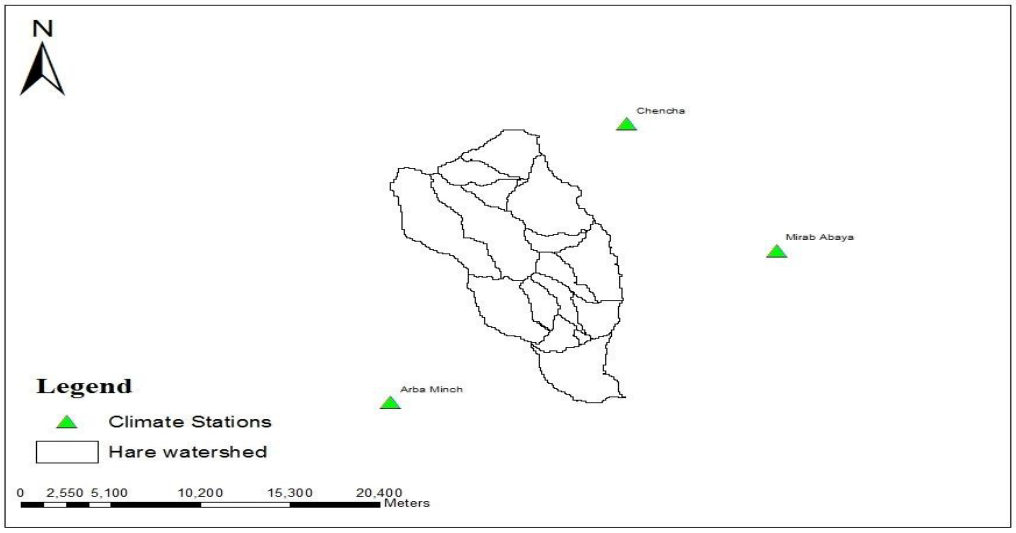


**Figure 2:** Location of climate station of Hare watershed.

| Stations | Grid Code | Corresponding output for the study area | |
|---|---|---|---|
| | | Latitude | Longitude |
| Arba Minch | GP111207 | 5.72 | 37.4 |
| Mirab Abaya | GP111208 | 6.16 | 37.4 |
| Chencha | GP111209 | 6.6 | 37.4 |

**Table 1:** Location of CORDEX-Ethiopia output grids for the study area [35].

precipitation amount P is transformed to a corrected $P^*$ a power transformation equation have been used.

$$P^*=aP^b \quad (1)$$

Where $P^*$ is the simulated data in the projection period, and a and b are the parameters obtained from calibration in the baseline period and subsequently applied to the projection period. They are determined by matching the mean and coefficient of variation (CV) of simulated data with that of observed data [16].

## Temperature correction

For temperature, monthly systematic biases were calculated for the baseline period by comparing RCPs outputs with the observations the monthly mean biases correction have been calculated according to the following Equation [17].

$$T_c = T_{om} + \frac{\delta_0}{\delta_r}\left(T_r - T_{rm}\right) \quad (2)$$

Where; $T_c$ is bias corrected future temperature, Tom is mean of observed temperature in base period, Trm is mean of RCPs temperature in base period and $T_r$ is RCPs temperature of base period $\delta_r$, and $\delta_0$, represent the standard deviation of the daily RCPs output and observations in the reference period respectively.

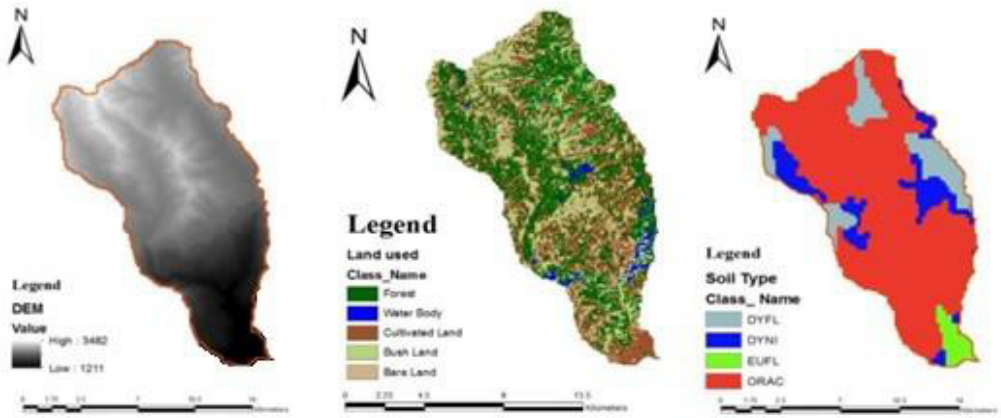


**Figure 3:** Spatial inputs of SWAT defined Dem, land use and soil type.

## Bias correction performance evaluation

The performance of the bias correction method was evaluated using the root means square error (RMSE), the mean absolute error (MAE) and the Relative Error (RE) [18]. They are calculated by the following equations (3), (4) and (5).

$$RMSE = \sqrt{\frac{\sum_{i}^{N}\left(Y_i^{'} - Y_i\right)^2}{N}} \quad (3)$$

$$MAE = \frac{1}{N}\sum_{i=1}^{N}\left|Y_i^{'} - Y\right| \quad (4)$$

$$RE = \frac{\frac{1}{N}\sum_{i=1}^{N}\left(Y_i^{'} - Y\right)}{Y_{mean}} \quad (5)$$

Where, $Y_i$ is the observed value at time step i, $Y_i$ is simulated value at time step i, $Y_{mean}$ is the mean of observed values, and N is the number of observations.

## Arc SWAT model approach

Watersheds can be subdivided into sub watersheds and further into hydrologic response units (HRUs) to account for differences in soils, land use, crops, topography, weather, etc. The model has a weather generator that generates daily values of precipitation, air temperature, solar radiation, wind speed, and relative humidity from statistical parameters derived from average monthly values. The model computes surface runoff volume either by using modified SCS curve number method or the Green and Ampt infiltration method. Flow is routed through the channel using a variable storage coefficient method or the Muskingum routing method. SWAT has three options for estimating potential evapotranspiration: Hargreaves, Priestley-Taylor, and Penman-Monteith. The model also includes controlled reservoir operation and groundwater flow model. The important equations used by the model are discussed below. The detailed and complete descriptions are given in the SWAT theoretical documentation. SWAT splits hydrological simulations of a watershed into two major phases: the land phase and the routing phase. The difference between the two lies on the fact that water storage and its influence on flow rates is considered in channelized flow [19].

## Weather generator

Lack of full and realistic long period climatic data is the problem of developing countries. Weather generators solve this problem by generating data having the same statistical properties as the observed ones [20]. SWAT requires daily values of precipitation, maximum and minimum temperature, solar radiation, relative humidity and wind speed. The climatic data collected from the three meteorological stations in the study area however, have too many missing data. As SWAT has a built-in weather generator called WGEN that is used to fill the gaps, all the missing values were filled with a missing data identifier, -99. The weather generator first independently generates precipitation for the day. Maximum temperature, minimum temperature, solar radiation and relative humidity are then generated based on the presence or absence of rain for the day. Finally, wind speed is generated independently [21].

For the sake of data generation, weather parameters were developed by using the weather parameter calculator WXPARM [22] and dew point temperature calculator DEW02 [23], which were downloaded from the SWAT website. The WXPARM program reads daily values of solar radiation (calculated from daily sunshine hours), maximum and minimum temperatures, precipitation, relative humidity, and wind speed data. It then calculates monthly daily averages and standard deviations of all variables as well as probability of wet and dry days, skew coefficient, and average number of precipitation days in the month. The DEW02 programs reads daily values of relative humidity, and maximum and minimum temperature values and calculates monthly average dew point temperatures [21].

## Hydrological component of SWAT

The simulation of the hydrology of a watershed is done in two separate divisions. One is the land phase of the hydrological cycle that controls the amount of water, sediment, nutrient and pesticide loadings to the main channel in each sub-basin. Hydrological components simulated in land phase of the hydrological cycle are canopy storage, infiltration, redistribution, evapotranspiration, lateral subsurface flow, surface runoff, ponds, tributary channels and return flow. The second division is routing phase of the hydrologic cycle that can be defined as the movement of water, sediments, nutrients and organic chemicals through the channel network of the watershed to the outlet. In the land phase of hydrological cycle, SWAT simulates the hydrological cycle

based on the water balance equation.

$$SW_t = SW_0 + \sum_{i=1}^{t}\left(R_{day} - Q_{surf} - E_a - W_{seep} - Q_{gw}\right)i \quad (6)$$

In which $SW_t$ is the final soil water content (mm), $SW_0$ is the initial soil water content on day i (mm), t is the time (days), $R_{day}$ is the amount of precipitation on day i (mm), $Q_{surf}$ is the amount of surface runoff on day i (mm), $E_a$ is the amount of evapotranspiration on day i (mm), $W_{seep}$ is the amount of water entering the vadose zone from the soil profile on day i (mm), and $Q_{gw}$ is the amount of return flow on day i (mm).

Using the above equation, the soil moisture content for the given area is simulated. Since the soil moisture storage is the main concern of this study, the brief description of some of the key model components are provided in this thesis. More detailed descriptions of the different model components are listed in Sallis et al. [19]. Soil water may follow different paths of movement: vertically upward (plant uptake), vertically downward (percolation), or laterally-contributing to stream flow. The vertical movement as plant uptake removes the largest portion of water that enters the soil profile.

The amount of soil water is usually measured in terms of water content as percentage by volume or mass, or as soil water potential, this soil water content is highly depending on the water balance values given in equation 6. Mostly, taking the precipitation as source of soil water content and reduction of run off, actual evapotranspiration, and ground water from precipitation is result in availability of water in the soil. Therefore, SWAT model revealed quantitatively the value of soil water content (SW) depends on the above water balance values.

However, water content does not necessarily describe the availability of the water to the plants, more indicates how the water moves within the soil profile. The only information provided by water content is the relative amount of water in the soil.

Soil water dynamics can be thought of as comparable to a sponge. When a sponge is saturated by soaking it in water when it is lifted out of the water, any excess water will drop off it. This is equivalent to drainage from the macro pores in the soil. Once the sponge has stopped dripping it is at field capacity.

When the sponge is squeezed, it is easy to get the first half of the water out. This first squeeze is equivalent to draining the sponge to the stress point and the water is removed like the RAWC (readily available water-holding capacity). Squeezing the second half of the sponge out is much harder. This is like draining the sponge to permanent wilting point. The total water squeezed out of the sponge from when it stopped dripping is the TAWC (Total Available Water-Holding Capacity). But no matter how hard the sponge is squeezed there is no way to get all the water out of it. The water left is the equivalent to the hygroscopic water found in soil. This sponge analogy is similar to how plant roots find getting moisture from the soil. From field capacity to the stress point it is easy to get the water. From the stress point to the permanent wilting point plants find it much harder to draw water from the soil and their growth is stunted. Below the permanent wilting point no further water can be removed and the plant dies [21].

**Percolation** is the downward movement of water in the soil. SWAT calculates percolation for each soil layer in the profile. Water is allowed to percolate if only the water content exceeds the field capacity of that layer [19].

**Surface runoff** occurs whenever the rate of precipitation exceeds the rate of infiltration. SWAT offers two methods for estimating surface runoff: the SCS curve number procedure and the Green and Ampt infiltration method [24]. Using daily or sub daily rain-fall, SWAT simulates surface runoff volumes and peak runoff rates for each HRU. In this study, the SCS curve number method was used to estimate surface runoff because of the unavailability of sub daily data for Green and Ampt method.

**Lateral flow** is common in areas with high hydraulic conductivities in surface layers and an impermeable or semi-permeable layer at a shallow depth. Rainfall will percolate vertically up to the impermeable layer and develops a saturated zone stored above this layer. This is called a perched water table, which is the source of water for lateral subsurface flow. SWAT incorporates a kinematic storage model for subsurface flow [19].

**The peak discharge** or the peak surface runoff rate is the maximum volume flow rate passing a particular location during a storm event. SWAT calculates the peak runoff rate with a modified rational method. In rational method, it assumed that a rainfall of intensity I begins at time t=0 and continues indefinitely, the rate of runoff will increase until the time of concentration, $t=t_{conc}$. The modified rational method is mathematically expressed as:

$$q_{peak} = \frac{\alpha tc * Q_{surf} * Area}{3.6 * t_{conc}} \quad (7)$$

Where, $q_{peak}$ is the peak runoff rate ($m^3/s$), αtc is the fraction of daily rainfall that occurs during the time of concentration, $Q_{surf}$ is the surface runoff (mm), Area is the sub-basin area ($km^2$), $t_{conc}$ is the time of concentration (hr), and 3.6 is a conversion factor.

**Potential evapotranspiration**: There are many methods that are developed to estimate Potential Evapotranspiration (PET). Three methods are incorporated into SWAT: The Penman-Monteith method [25], the Priestley-Taylor method and the Hargreaves method [26]. For this study, Penman-Monteith method were used.

**Groundwater:** The simulation of groundwater is partitioned into two aquifer systems i.e., an unconfined aquifer (shallow) and a deep-confined aquifer in each sub basin. The unconfined aquifer contributes to flow in the main channel or reach of the sub basin. Water that enters the deep aquifer is assumed to contribute to stream flow outside the watershed [27]. In SWAT the water balance for a shallow aquifer is calculated with equation 8.

$$aq_{sh,i} = aq_{sh,i-1} + W_{rchrg} + Q_{gw} - W_{deep} - W_{pump,sh}$$

where: $aq_{sh,i}$ is the amount of water stored in the shallow aquifer on day i (mm), $aq_{sh,i-1}$ is the amount of water stored in the shallow aquifer on day i-1 (mm), $W_{rchrg}$ is the amount of recharge entering the aquifer on day i (mm), $Q_{gw}$ is the groundwater flow, or base flow, into the main channel on day i (mm), $WR_{evap}$ is the amount of water moving into the soil zone in response to water deficiencies on day i (mm), $W_{deep}$ is the amount of water percolating from the shallow aquifer into the deep aquifer on day i (mm), and $W_{pump,sh}$ is the amount of water removed from the shallow aquifer by pumping on day i (mm).

## SWAT Model Setup

### Watershed delineation

Watershed delineator tool in Arc SWAT allows the user to delineate the watershed and sub-basins using DEM. Flow direction and accumulation are the concepts behind to define the stream network of

the DEM in SWAT. The monitoring point is added manually and the numbers of sub-basin are adjusted accordingly. Finally, the catchment area is delineated to be 153 km$^2$ for Hare River catchment, and 17 sub-basins are formed for the whole catchment.

### HRU analysis

HRU analysis helps to load land use map and soil map and also incorporates classification of HRU into different slope classes. The land use map as well as soil map was overlapped 100% with the delineated watershed and 103 HRUs were formed for the study area. Spatial inputs of slope, soil, and land use were used to define the catchment. 30-meter resolution of USGS DEM topographic data was used for slope classification. Extracted topographic map with the catchment boundary shows an elevation range from 1211 to 3482 m amsl.

### Weather data definition

Available meteorological records (1980-2006) (i.e., precipitation, minimum and maximum temperatures, relative humidity, and wind speed) and location of meteorological station are prepared based on Arc SWAT input format and integrated with the model using weather data input wizards. Arba Minch meteorological station data were used as weather generator for this study.

### Sensitivity analysis

Sensitivity analysis is a technique of identifying the responsiveness of different parameters involving in the simulation of a hydrological process. For big hydrological models like SWAT, which involves a wide range of data and parameters in the simulation process, calibration is quite a cumbersome task. Even though, it is quite clear that the flow is largely affected by curve number, for example in the case of SCS curve number method, this is not sufficient enough to make calibration as little change in other parameters could also change the volumetric, spatial, and temporal trend of the simulated flow. Hence, sensitivity analysis is a method of minimizing the number of parameters to be used in the calibration step by making use of the most sensitive parameters largely controlling the behavior of the simulated process. This appreciably eases the overall calibration and validation process as well as reduces the time required for it. Besides, as Dutra et al. [28] indicated, it increases the accuracy of calibration by reducing uncertainty.

The sensitivity analysis was undertaken by using a built-in tool in SWAT that uses the Latin Hypercube One-factor-At-a-Time (LH-OAT). Details of this method are explained in Robinson et al. [29]. After the analysis, the mean relative sensitivity (MRS) of the parameters was used to rank the parameters, and their category of Dutra et al. [28] classification. He divided sensitivity was also defined based on the sensitivity into four classes as shown in Table 2. Eime et al. [4] indicated that there can high (0.20) be a significant variation of hydrological processes between individual watersheds. This, therefore, justified the need for the sensitivity analysis made in the study area. The analysis involved a total of 28 parameters. For the study area, the sensitivity analysis should be carried out for a period of twelve years, which included both calibration period (from January 1, 1993 to December 31, 2002) and the warm-up period (From January 1, 1991 to December 31, 1992).

### Model calibration and validation

Calibration is tuning of model parameters based on checking results against observations to ensure the same response over time. This involves comparing the model results, generated with the use of historic meteorological data, to recorded stream flows. In this process, model parameters varied until recorded flow patterns are accurately simulated. Model calibration of SWAT run can be divided in to several steps. Among these Water balance and stream flow generation are the most important part is also considered.

Ref. [19] distinguished three types of calibration methods: the manual trial-and-error method, automatic or numerical parameter optimization method; and a combination of both methods. According to the authors, the manual calibration is the most common and especially recommended in cases where a good graphical representation is strongly demanded for the application of more complicated models. However, it is very cumbersome, time consuming, and requires experience. Automatic calibration makes use of a numerical algorithm in the optimization of numerical objective functions. The method undertakes a large number of iterations until it finds the best parameters. The third method makes use of combination of the above two techniques regardless of which comes first. For this study, the first and the third approach was considered [30].

The manual calibration of this study was done based on the procedures recommended in SWAT user manual. Water balance calibration normally takes care of the overall flow volume and its distribution among the different hydrologic components, whereas temporal flow calibration is concerned about the flow time lag and the hydrograph shape [21]. For this case study also, as the soil moisture data is not available at the station, one of the water balance component with observed data, (stream flow) is used for calibration and validation purpose. The automatic calibration was done using Parameter Solution (Parasol) [4]. This method was chosen for its applicability to both simple and complex hydrological models.

Calibration for water balance and stream flow is first done for average annual conditions. Once the model is calibrated for average annual conditions, it can be repeated to monthly or daily records to fine-tune the calibration. Accordingly, the annual and monthly calibration was taken for the study area. Flow calibration was performed for a period of ten years from January 1, 1993 to December 31, 2002 using the sensitive parameters identified. However, flow was simulated for twelve years from January 1, 1991 to December 31, 2002, within which the first two year was considered as a warm up period. Flow validation was performed for a period of four years from January 1, 2003 to December 31, 2006.

The flow was calibrated manually using the observed flow gauged at the outlet of the watershed. First of all, the surface runoff flow components of gauged flow were balanced with that of the simulated flow.

Afterwards the adjusted flow was further calibrated temporally by making delicate adjustments to ensure best fitting of the simulated flow curves with the gauged flow curves. Manipulation of the parameter values were carried out within the allowable ranges recommended by SWAT developers. The factor of goodness fit can be quantified by the coefficient of determination ($R^2$) and Nash-Sutcliff efficiency (NSE) between the observations and the final best simulations. Coefficient of determination ($R^2$) and Nash-Sutcliffe coefficient (NSE) are calculated by:

$$R^2 = \frac{\left[\left(\sum_i Q_{m,i} - \bar{Q}_m\right)\left(Q_{s,j} - \bar{Q}_s\right)\right]^2}{\left(\sum_i Q_{mi,j} - \bar{Q}_m\right)^2 \sum_i \left(Q_{s,i} - \bar{Q}_s\right)^2} \quad (9)$$

$$NSE = 1 - \frac{\sum_i (Q_m - Q_s)i^2}{\sum_i (Q_{m,i} - Q_m)^2} \quad (10)$$

In which $Q_m$ is the measured discharge, $Q_s$ is the simulated discharge, $\overline{Q}_m$ is the average measured discharge and $\overline{Q}_s$ is the average simulated discharge.

### Hydrologic impact of future climate change scenario

The main objective of downscaling is to generate a reliable estimation of meteorological variables corresponding to given scenario of the future climate so that these meteorological variables will be used as basis for different types of impact studies. Therefore, after calibration and validation of hydrological models with historical record, the next step in the investigation is to simulate river flows in the watershed corresponding to future climate conditions by using the downscaled precipitation and temperature in to SWAT model. Such simulation helps to identify the hydro climatological impacts caused by climate change.

The future climate variables that is downscaled precipitation and temperature found as an output from the RCPs and corrected RCPs were given as an input to the SWAT model. Then simulation results corresponding to each of downscaling scenario time period (current, 2020s, 2050, and 2080s) are analyzed for all month of the year.

## Results and Discussion: Bias Correction Results

In this study, the bias correction method was applied to simulate climate variables: precipitation for three meteorological stations (Arba Minch, Chencha and Mirab Abaya) and maximum temperature and minimum temperature for Arba Minch station.

The results of the bias correction method were evaluated using residual plots (difference between the simulated and observed values) of precipitation and temperature in terms of mean. Standard model performance statistics tests were carried out by computing the root mean square error (RMSE), the mean absolute error (MAE) and the relative error (RE).

The monthly residuals of bias corrected climate variables (precipitation, maximum temperature, and minimum temperature) are presented in Figure 4. The figures show that a significant improvement is achieved by applying bias correction method on RCPs since the bias corrected results provided smaller monthly mean bias values than the raw RCPs results. In other words, the bias corrected results are closer to the observed values than the raw RCPs results at the three stations.

As shown in the Figure 4a, the mean monthly residuals of raw precipitation are between -83.1 mm and +62.8 mm and after bias correction the residuals are between -13.6 mm and +0.01 mm. Figure 4b shows that, the mean monthly residuals of raw precipitation are between -738.1 mm and +34.7 mm and after bias correction the residuals are between -11.7 mm and +17.7 mm. Figure 4c shows that, the mean monthly residuals of raw precipitation are between -49.8 mm and +56.1 mm and after bias correction the residuals are between -37.5 mm and +0.02 mm which indicates that significant improvement is achieved after bias correction.

Again, for Arba Minch station, the bias corrected mean daily maximum temperature and minimum temperature was compared with the raw mean daily maximum temperature and minimum temperature using residual plots.

As shown in the Figure 5a and 5b the mean daily residual plots of raw and bias corrected mean daily maximum temperature and minimum temperature. It is found that while the raw mean daily maximum temperature residuals are between -1.5°C and +1.4°C, after bias correction the range is between -1.1°C and +1°C in terms of mean and raw mean daily minimum temperature residuals are between -2.3°C and +3.4°C, after bias correction the range is between -1.4°C and +2.1°C in terms of mean.

The bias corrected results show that the corrected RCPs provided fewer errors than the raw RCP results. From Table 3, it can be seen that the models' performance (RMSE, MAE, and RE) for precipitation, maximum temperature, and minimum temperature was good and almost the same.

### Future climate projection precipitation

The rainfall expected to experience a mean monthly increase by 6.40, 2.56, and 16.30% for RCP4.5 scenario at 2020s, 2050s, and 2080, respectively. The mean annual increase was repeated by RCP8.5 scenario with 8.56, 8.08, and 15.85% at 2020s, 2050s, and 2080s, respectively. These values show that increasing in rainfall is not uniform; instead, it differs from time period to time period

A mean monthly rainfall projection of Kiremt (Jun-September) increase by 1.79, 1.43, and 1.68% for RCP4.5 scenario and RCP8.5 scenario by 4.10, 3.96, and 12.52% at 2020s, 2050s, and 2080, respectively and Bega (October-January) shows increasing by 18.91, 21.46, and 58.84% for RCP4.5 scenarios and RCP8.5 scenarios by 31.52, 37.42, and 56.00% at 2020s, 2050, and 2080s, respectively. A mean monthly rainfall projection of Belg (February-May) decrease by 1.50, 15.20, and 16.77% for RCP4.5 scenario and RCP8.5 scenario by 9.94, 17.14, and 20.97% at 2020s, 2050s, and 2080, respectively. A rainfall projection of Kiremt (Jun-September) and Bega (October-January) shows increasing the two emission scenarios whereas Belg (February-May) projection shows a decreasing mean monthly rainfall for the two emission scenarios (Figure 6a and 6b).

Percentage change in monthly, seasonal, and annual precipitation for the period 2010-2099 generally increasing during the Kiremit (wet season=June–September) for the long-term future and also indicate a corresponding increase in precipitation for the Belg (less rainy season=February-May) for 2050s and 2080s [31].

### Maximum temperature

The projected mean monthly maximum temperature shows increasing trend for all time periods by 0.01, 0.02, and 0.11°C for RCP4.5 scenario for 2020s, 2050s, and 2080, respectively. RCP8.5 scenario also shows an increase of mean monthly maximum temperature with 0.01, 0.03, and 0.11°C for 2020s, 2050s and 2080s, respectively. As compared to RCP8.5 scenario, RCP4.5 scenario is almost the same (Figure 7a and 7b).

### Minimum temperature

The projected minimum temperature shows an increasing trend in all time periods. In this case, both the RCP4.5 and RCP8.5 emission scenarios predict the future minimum temperature in similar manner. For RCP4.5 scenario, mean monthly minimum temperature increases by 0.06, 0.07, and 0.12°C and for RCP8.5 scenario 0.32, 0.15, and 0.13°C for 2020s, 2050s, and 2080s, respectively. Mean monthly variation of minimum temperature is higher than maximum temperature (Figure 8a and 8b).

According to the Ethiopian National Meteorological Services

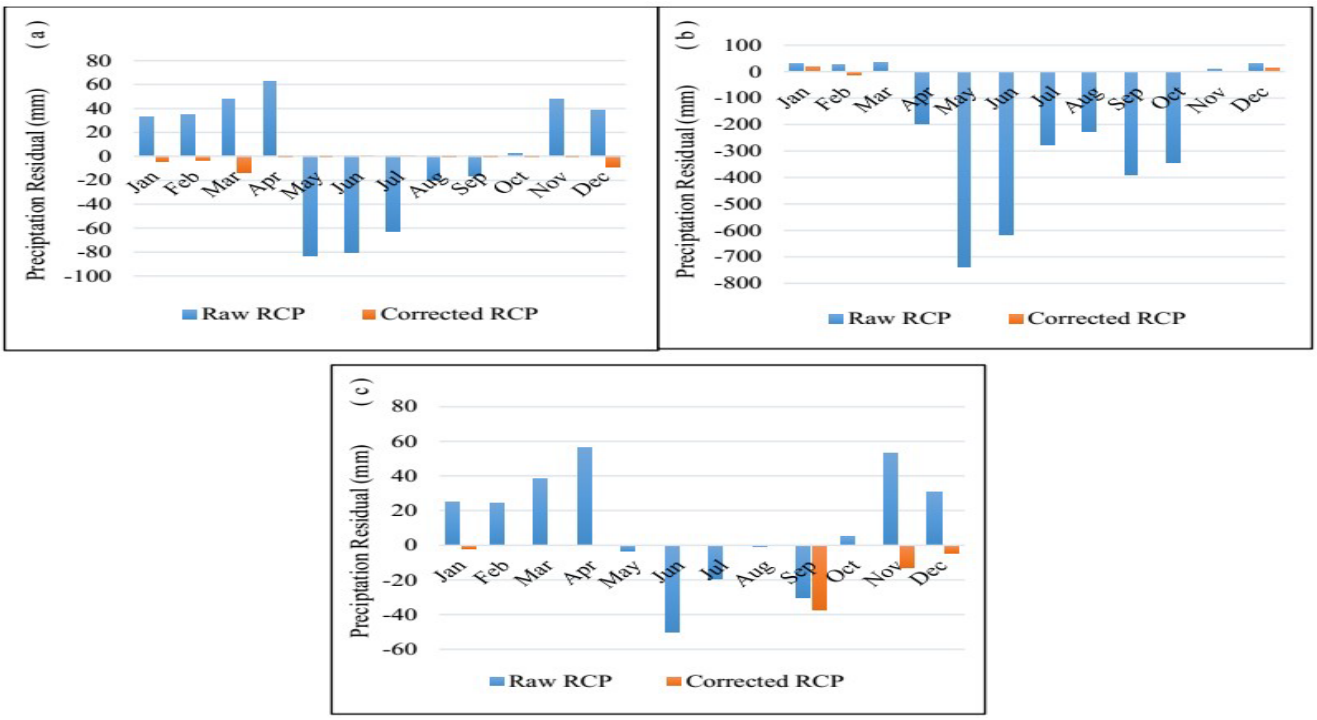


**Figure 4:** Mean monthly residuals of raw RCPs and corrected RCPs (1980-2006) a) Arba Minch, b) Chencha and c) Mirab Abaya.

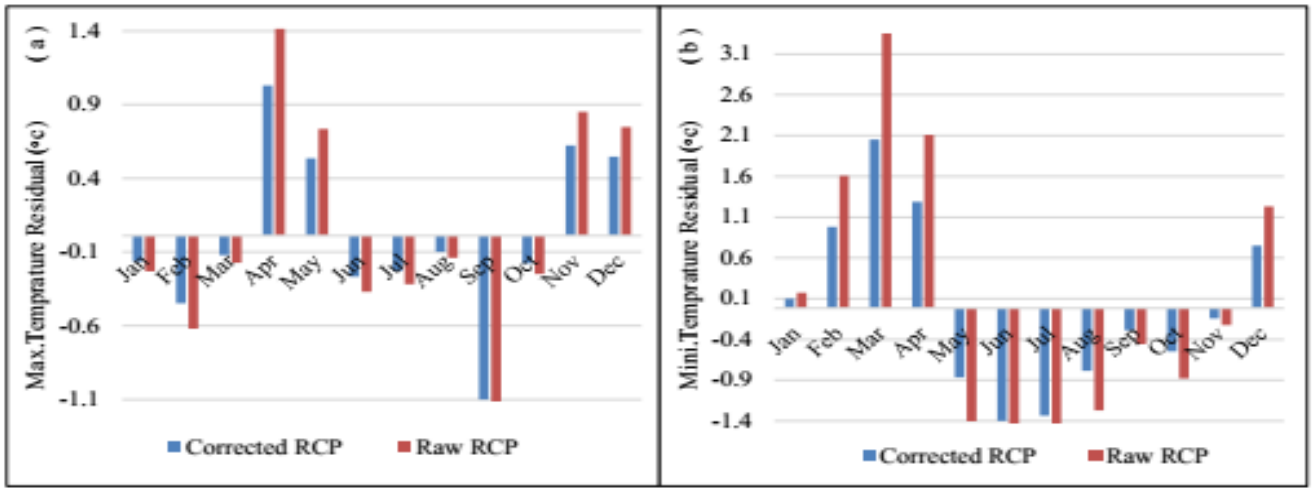


**Figure 5:** Mean monthly residuals temperature of raw RCPs and corrected RCPs (1980-2006) at Arba Minch.

| Class | Index | Sensitivity |
|---|---|---|
| I | 0.00≤/I/<0.05 | Small to Negotiable |
| II | 0.05≤/I/<0.2 | Medium |
| III | 0.2≤/I/<1 | High |
| IV | /I/≥1 | Very high |

**Table 2:** Sensitivity Class for SWAT model Source: [28].

Agency [5] the study for 40 stations showed that there have been very warm and very cold years. However, the general trend showed there was an increase in temperature over the last 50 years. The study also noted that the minimum temperature is increasing at a higher rate than the maximum temperature.

## Hydrological model calibration and validation

In this study, soil, and water assessment hydrological tool (SWAT) model were employed to simulate streamflows for Hare river watershed using observed and bias corrected precipitation and temperature data.

As mentioned in the methodology part, flow sensitivity analysis has been carried out for 26 hydrological parameters using SWAT sensitivity analysis. The most sensitive parameters considered for calibration were Curve number (CN2), Soil Evaporation Compensation factor (ESCO), Groundwater recession factor (ALPHA_BF), Soil Available Water Capacity (SOL_AWC), Soil depth (SOL_Z), Saturated hydraulic conductivity (SOL_K), Slope (SLOPE), Threshold depth of water in

| Station | Evaluation | Precipitation | Temperature Max | Temperature Min |
|---|---|---|---|---|
| Arba Minch | RMSE | 12.29 | 1.76 | 1.46 |
| | MAE | 1.69 | 0.0629 | 0.0672 |
| | RE | 0.0329 | $2.6 \times 10^{-15}$ | 0.0238 |
| Chencha | RMSE | 9.36 | - | - |
| | MAE | 1.49 | - | - |
| | RE | -0.0156 | - | - |
| Mirab Abaya | RMSE | 10.55 | - | - |
| | MAE | 1.76 | - | - |
| | RE | 0.077 | - | - |

**Table 3:** Performance statistics of bias correction method.

the shallow aquifer required for return flow occur (GWqmn), Ground water delay (GW_DELAY), Average slope length (SLSUBBSN) and Plant evaporation compensation factor (EPCO). Result of sensitivity analysis was used to conduct the calibration of SWAT. The calibration was performed with the seven sensitive parameters of stream flow. After several iterations, fitted values for the seven parameters were gained (Table 4).

Performance of the best simulation of stream flow result which used these fitted parameter values for calibration and validation is shown in Table 5. Govindan et al. [30] stated that Nash–Sutcliff efficiency (NSE) values greater than or equal to 0.50 are considered adequate for SWAT model application. Hence, it is observed that SWAT exhibited strong performance in representing the hydrological conditions of the catchment. It can be seen from the flow hydrographs (Figure 9a and 9b) that the simulated flows well matched the observed flows except for peak values in the calibration period and low values in the validation period for both daily and monthly time steps.

## Simulation of hydro climatological impacts caused by climate change

One of the main objectives of this study was simulation of hydro climatological impacts caused by climate change over the study area. Therefore, this section of result and discussion is one of the ultimate goals of this study. For this purpose, the changes of downscaled climate variables (temperature and precipitation) from the baseline climate were used to get 2020s, 2050s, and 2080s (each has 30 years daily climatic data including the baseline) time series data. SWAT simulation was run four times (for the baseline, 2020s, 2050s, and 2080s) by keeping constantly calibrated soil, crop, and slope parameters to quantify climate change impact only. Simulation results of stream flow for the three future time periods, 2020s, 2050s, and 2080s, were compared with the baseline period simulation.

Mean monthly stream flow may increase by 12.2, 8.0, and 13.9% for 2020s, 2050s, and 2080s, respectively, from the baseline stream flow for RCP4.5 scenario whereas for RCP8.5 scenario, the model shows an increase by 7.3, 13.4, and 15.4% for 2020s, 2040s, and 2080s, respectively (Figure 10a and 10b).

The same streamflow metrics used for assessing the effects land use change were also used for assessing the effects of climate change. Consistent with other research [8,32,33], the climate only scenarios had a larger effect on streamflow than land use change. In 2050s, mean annual streamflow is found to increase in all the scenarios. The maximum projected increase in discharge of 32.46% was found for

| Rank | Parameter | SWAT default | | Fitted Value |
|---|---|---|---|---|
| | | Lower bound | Upper bound | |
| 1 | CN2 | 35 | 98 | 64 to 85 |
| 2 | ESCO | 0 | 1 | 9.5 |
| 3 | ALPHA_BF | 0 | a | 0.06 |
| 4 | SOL_AWC | 0 | 1 | 0.01 to 0.30 |
| 5 | SOL_Z | 0 | 3000 | 200 to 490 |
| 6 | SOL_K | 0 | 100 | 4.3 to 80 |
| 7 | SLOPE | 0 | 1 | 0.06 to 0.75 |
| 8 | GWqmn | 0 | 5000 | 50 |
| 9 | GW_DELAY | 0 | 50 | 20 |
| 10 | SLSUBBSN | 10 | 150 | 10 to 43 |
| 11 | EPCO | 0 | 1 | 0.85 |

**Table 4:** Calibrated fitted values of flow-sensitive parameters.

| Criteria | Calibration (1991-2002) | Validation (2003-2006) |
|---|---|---|
| Coefficient of determination ($R^2$) | 0.85 | 0.84 |
| Nash-Sutcliffe efficiency (NSE) | 0.73 | 0.77 |

**Table 5:** Calibrated model simulation performance.

GISSE2-H (RCP 4.5), ware as MIROC-ESMCHEM (RCP 8.5) and BCC-CSM1.1

(RCP 8.5) showed almost same increase in projected annual discharges which are 26.89% and 26.27% consecutively. In 2080s, the maximum projected increase in discharge of 47.44% was found for BCC- CSM1.1 (RCP 8.5). Other scenarios gave variable increase in discharge, 29.50%, 18.96%, 38.82% and 13.60% increase in mean annual streamflow were found for MIROC-ESMCHEM (RCP 8.5), HADGEM2- ES (RCP 8.5), GISS-E2-H (RCP 4.5) [34].

## Conclusions and Recommendations

The bias correction for downscaled RCPs data, the raw RCPs data was corrected by a bias correction methods successfully as the simulated climate variables produced consistent results with the historical records. The residuals between corrected and historical monthly values were smaller than the residuals between raw RCP and historical monthly values of precipitation and temperature. The models' evaluation of performance for precipitation, maximum temperature, and minimum temperature was good and almost the same. The bias correction method the most accurate method for downscaled climate variables to reproducing the main features of the observed data.

The rainfall projection expected to experience a mean monthly increase by 6.40, 2.56, and 16.30% for RCP4.5 scenario at 2020s, 2050s, and 2080, respectively. The mean annual increase was repeated by RCP8.5 scenario with 8.56, 8.08, and 15.85% at 2020s, 2050s, and 2080s, respectively. For both RCPs scenarios, the maximum and minimum temperature projection expected increasing for all future period.

The simulations were done using the IPCC RCP4.5 and RCP8.5 emission scenario. The curve number, Soil Evaporation Compensation factor (ESCO), and Alfa base flow parameter showed a relatively very higher sensitivity. Soil water assessment tool (SWAT) models were well calibrated and validated using observed flow data as the coefficient determination was above 0.7 and Nash Sutcliffe efficiency index was above 0.5 for watershed.

Mean monthly percentage changes of climate variables from the baseline period were used to simulate future projections of stream

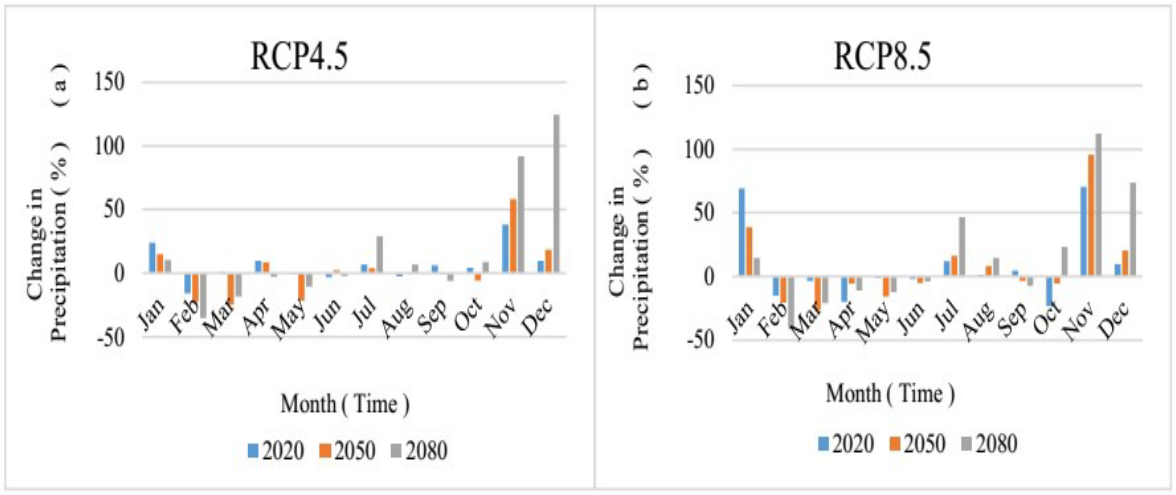


**Figure 6:** Future changes in mean monthly precipitation for a) RCP4.5 and b) RCP8.5 scenarios.

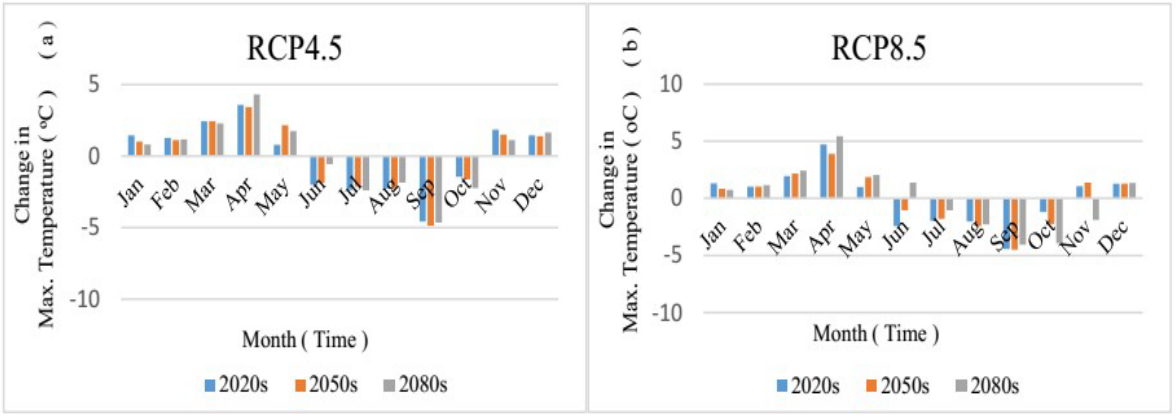


**Figure 7:** Future changes in mean monthly Maximum temperature for a RCP4.5 and b RCP8.5 scenarios.

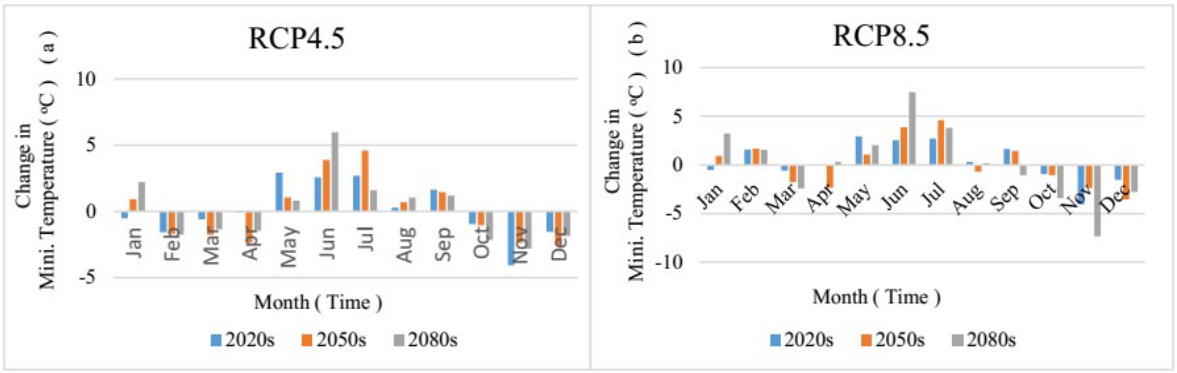


**Figure 8:** Future changes in mean monthly Minimum temperature for a RCP4.5 and b RCP8.5 scenarios.

flow. Stream flow projections for future time periods showed that mean monthly stream flow may increase by 12.2, 8.0, and 13.9% at 2020s, 2050s, and 2080s, respectively, from the baseline period for RCP4.5 scenario, whereas for RCP8.5 scenario, it will be expected to increase by 7.3, 13.4, and 15.4% for 2020s, 2040s, and 2080s, respectively.

Data quality and availability should be stressed much more while using distributed hydrological models. The applications SWAT models were very challenging and a lack of appropriate data was one of the biggest concerns throughout. Without proper data, model implementation is very difficult if not impossible.

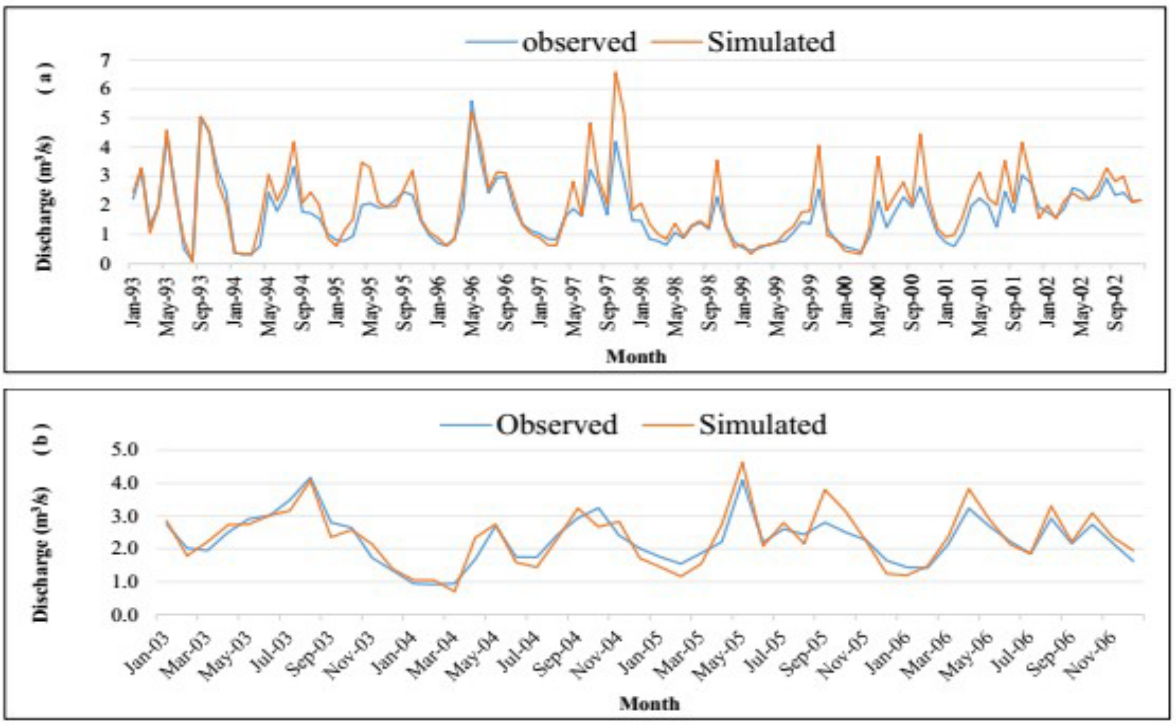


**Figure 9:** a) Calibration and b) Validation result of average monthly simulated and gauged flows.

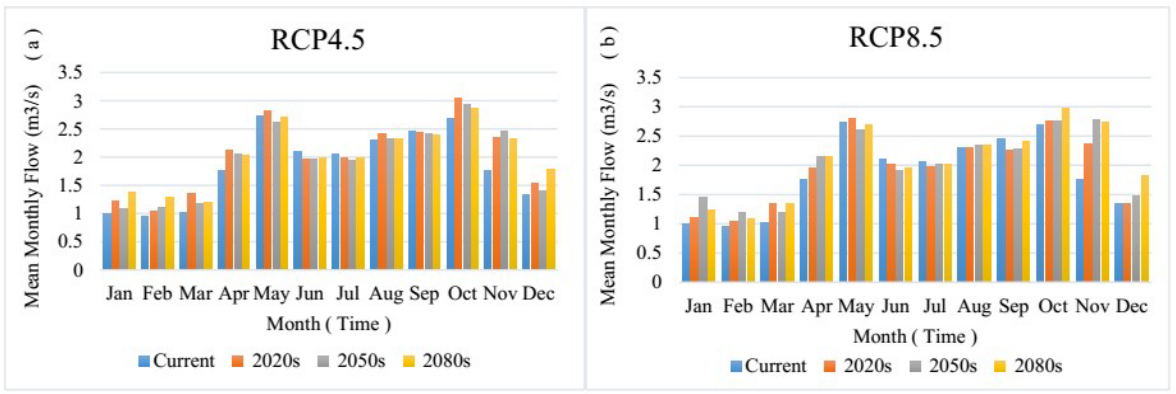


**Figure 10:** Mean monthly flow for a RCP4.5 and b RCP8.5 scenarios.

The model simulations considered only future climate change scenarios assuming all spatial data constant. But change in land use scenarios other climate variables will also contribute some impacts on future stream flow.

Uncertainty analysis is recommended to assess the uncertainty associated with the bias correction method, the hydrological models, and the RCPs. Finally, to link the study results to the sustainable development of the community, it is recommended to use the hydrological models' outputs in water resource management models to take the socio-economic aspects of the hydrological system [35-39].

## Acknowledgements

I would also like to thank the Ministry of Water Irrigation and Energy, Ministry of Agriculture and National Meteorological Services Agency of Ethiopia for providing me discharge, soil and climate data respectively.

## References

1. Salvi K, Kannan S, Ghosh S (2011) Statistical Downscaling and Bias Correction for Projections of Indian Rainfall and Temperature in Climate Change Studies. 2011 International Conference on Environmental and Computer Science 19: 7-11.
2. IPCC-TGICA (2007) General Guidelines on the Use of Scenario Data for Climate Impact and Adaptation Assessment. Version 2, Prepared by Carter TR on behalf of the Intergovernmental Panel on Climate Change, Task Group on Data and Scenario Support for Impact and Climate Assessment, p: 66.
3. Frederick KD (2002) Introduction. In: Water resource and climate change. Fredrick KD (ed.), Northampton MA, Edward Elgar Publishing, p: 514.
4. Van Griensven A, Meixner T, Grunwald S, Bishop T, Diluzio M, et al. (2006) A global sensitivity analysis tool for the parameters of multi-variable catchment models. Journal of Hydrology 324: 10-23.
5. NMSA (National Meteorological Service Agency) (2001) Initial National Communication of Ethiopia to the United Nations Framework convention on Climate Change (UNFCCC). National Meteorological Services Agency.

6. Kassa TM (2009) Watershed hydrological responses to changes in land use and land cover, and management practices at hare watershed, Ethiopia.
7. Förch G (2007) Assistance to Arba Minch Water Technology Institute (AWTI). A Brief History of German Project Support and its Impacts on the Ethiopian and German Partners. Proceedings of Lake Abaya Research Symposium (LARS), FWU Water Resources Publication, p: 6.
8. Caldwell PV, Sun G, McNulty SG, Cohen EC, Myers JM (2012) Impacts of impervious cover, water withdrawals, and climate change on river flows in the conterminous US. Hydrology and Earth System Sciences 16: 2839-2857.
9. Moss RH, Edmonds JA, Hibbard KA, Manning MR, Rose SK, et al. (2010) The Next Generation of Scenarios for Climate Change Research and Assessment. Nature 463: 747-756.
10. Stocker TF, Qin D, Plattner GK, Tignor M, Allen SK, et al. (2013) Climate Change 2013: The Physical Science Basis. Contribution of Working Group I to the Fifth Assessment Report of the Intergovernmental Panel on Climate Change. Cambridge University Press, Cambridge, United Kingdom and New York, NY, USA, p: 1535.
11. FAO (1998) The Soil and Terrain Database for northeastern Africa (CDROM) FAO, Rome.
12. FAO (Food and Agricultural Organization) (2002) Major Soils of the World. Land and Water Digital Media Series. FAO Soil Buletin No 19, Rome, Italy.
13. FAO (1995) Digital Soil Map of the World and Derived Soil Properties (CDROM) Food and Agriculture Organization of the United Nations, FAO.
14. Van Wambeke A (2003) Properties and management of soils of the tropics. FAO Land and Water Digital Media Series No. 24, FAO, Rome.
15. Gebrie GS, Engida AN (2015) Climate Modeling of the Impact of Climate Change on Sugarcane and Cotton for Project on 'a Climate Resilient Production of Cotton and Sugar in Ethiopia.
16. Leander R, Buishand TA (2007) Resampling of regional climate model output for the simulation of Extreme River flows. J Hydrol 332: 487-496.
17. Ho CK, Stephenson DB, Collins M, Ferro CAT, Brown SJ (2012) Calibration Strategies A Source of Additional Uncertainty in Climate Change Projections. Bulletin of the American Meteorological Society 93: 21-26.
18. Shamarokh A (2012) Hydrological Impact of Climate Change in Semi-Urban Watershed. MSc Thesis, Civil and Environmental Engineering (Bangladesh Univ of Engg. & Tech.).
19. Neitsch SL, Arnold JG, Kiniry JR, Williams JR (2005) Soil and Water Assessment Tool, Theoretical Documentation: Version 2005. Temple, TX. USDA Agricultural Research Service and Texas A & M Black Land Research Centre.
20. Danuso F (2002) Climak. A Stochastic Model for Weather Data Generation. Italian Journal of Agronomy 6: 57-71.
21. Yakob M (2009) Climate change impact assessment on soil water availability and crop yield in anjeni watershed Blue Nile basin. A Thesis Submitted to School of Graduate Studies Arba Minch University in Partial Fulfillment of the Requirement for the Degree of Master of Science in Meteorology.
22. Williams JR (1969) Flood routing with variable travel time or variable storage coefficients. Trans ASAE 12: 100-103.
23. Liersch S (2003) The Programs dew.exe and dew02.exe User's Manual. Berlin, p: 5.
24. Green WH, Ampt GA (1911) Studies on soil physics: 1. The flow of air and water through soils. J Agric Sci 4: 11-24.
25. Monteith JL (1965) Evaporation and the environment. In the State and Movement of Water in living Organisms. XIXth Symposium Soc For Exp Biol, Swansea, Cam-bridge University Press, pp: 205-234.
26. Hargreaves GL, Hargreaves GH, Riley JP (1985) Agricultural benefits for Senegal River basin. J Irrig and Drain Engr 111: 113-124.
27. Arnold JG, Allen PM, Bernhardt G (1993) A comprehensive surface-groundwater flow model. Journal of Hydrology 142: 47-69.
28. Lenhart T, Eckhardt K, Fohrer N, Frede HG (2002) Comparison of two different approaches of sensitivity analysis. Physics and Chemistry of the Earth 27: 645-654.
29. Huisman S, Griensven AV, Srinivasan R, Breuer L (2004) European SWAT School, Advanced Course, p: 112 (Institute for Landscape Ecology and Resource Management, University of Giessen, Hienrich-BuffRing 26, 35392 Giessen, Germany).
30. Santhi C, Arnold JG, Williams JR, Dugas WA, Srinivasan R, et al. (2001) Validation of the SWAT Model on a Large River Basin with Point and Non-Point Sources. Journal of the American Water Resources Association 37: 1169-1188.
31. Dile YT, Berndtsson R, Setegn SG (2013) Hydrological Response to Climate Change for Gilgel Abay River, in the Lake Tana Basin-Upper Blue Nile Basin of Ethiopia. PLoS ONE 8: e79296.
32. Lockaby G, Nagy C, Vose JM, Ford CR, Sun G, et al. (2013) Forests and water. In: The Southern Forest Futures Project: Technical Report. SRSGTR-178. USDA-Forest Service, Southern Research Station, Asheville, NC, USA.
33. Sun G, McNulty SG, Myers JA, Cohen EC (2008) Impacts of Multiple Stresses on Water Demand and Supply Across the Southeastern United States. Journal of the American Water Resources Association 44: 1441-1457.
34. Sarfaraz A (2015) Impact of climate change on future flow of Brahmaputra river basin using swat model. MSc Engineering Thesis, Department of Water Resources Engineering, Bangladesh University of Engineering and Technology (BUET), Dhaka.
35. Biniyam Y, Kemal A (2017) The Impacts of Climate Change on Rainfall and Flood Frequency: The Case of Hare Watershed, Southern Rift Valley of Ethiopia. J Earth Sci Clim Change 8: 383.
36. Chalise SR (1994) Mountain Environments and Climate Change in the Hindu Kush- Himalayas. In: Beniston M (ed.), Mountain Environments in Changing Climates, Routledge, London, UK, pp: 383-404.
37. Refsgaard JC, Storm B (1996) MIKESHE. In: Computer Models in Watershed Hydrology. Singh VJ (ed.), Highland Ranch, Colo: Water Resources Publications, pp: 809-846.
38. Ho CK, Stephenson DB, Collins M, Ferro CAT, Brown SJ (2015) Calibration Strategies a Source of Additional Uncertainty in Climate Change Projections. Bull Amer Met Soc 93: 21-26.
39. Wurbs RA, Muttiah RS, Felden F (2005) Incorporation of climate change in water availability modeling. Journal of Hydrologic Engineering 10: 375-385.